

## **Interaction of Uranium(VI) with $\alpha$ -Amylase and Its Implication for Enzyme Activity**

Barkleit, A.; Hennig, C.; Ikeda-Ohno, A.;

Originally published:

September 2018

**Chemical Research in Toxicology 31(2018), 1032-1041**

DOI: <https://doi.org/10.1021/acs.chemrestox.8b00106>

Perma-Link to Publication Repository of HZDR:

<https://www.hzdr.de/publications/Publ-27359>

Release of the secondary publication  
on the basis of the German Copyright Law § 38 Section 4.

# **Interaction of uranium(VI) with $\alpha$ -amylase and its implication for the enzyme activity**

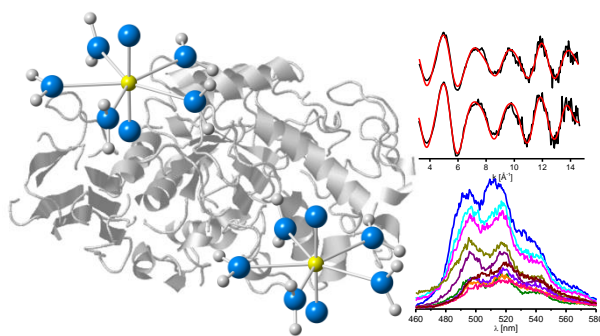
Astrid Barkleit\*, Christoph Hennig, and Atsushi Ikeda-Ohno

*Helmholtz-Zentrum Dresden - Rossendorf, Institute of Resource Ecology,*

*Bautzner Landstraße 400, 01328 Dresden, Germany*

*\* Corresponding author. E-mail: a.barkleit@hzdr.de, phone: +49 351 260 3136*

## Table of Contents (TOC)



## Abstract

Due to its chemo- and radiotoxicity, the incorporation of uranium into human body via ingestion potentially poses a serious health risk. When ingested, the gastrointestinal fluids are the primary media to interact with uranium, eventually influencing and even determining its biochemical behavior in the gastrointestinal tract and thereafter. The chemical interactions between uranium and the components of gastrointestinal fluids are, however, poorly understood to date. In this study, the complexation of uranium(VI) (as the uranyl ion,  $\text{UO}_2^{2+}$ ) with the protein  $\alpha$ -amylase, one of the major enzymes in saliva and pancreatic juices, was investigated over a wide range of pH or uranium/  $\alpha$ -amylase concentrations covering physiological conditions. Macroscopic sorption experiments suggested a strong and fast complexation of  $\text{UO}_2^{2+}$  to  $\alpha$ -amylase between pH 5 and 7. Potentiometric titration was employed to determine the complex stability constants for the relevant  $\text{UO}_2^{2+}$   $\alpha$ -amylase complexes, which is crucial for reliable thermochemical modeling to assess the potential health risk of uranium. Extended X-ray absorption fine structure (EXAFS) spectroscopy revealed that  $\alpha$ -amylase is interacting with  $\text{UO}_2^{2+}$  primarily via its carboxylate groups presumably from the aspartic acid and glutamic acid side chains. The effect of  $\text{UO}_2^{2+}$  on the enzyme activity was also investigated to understand the potential implication of uranium for the *in vivo* functions of the digestive fluids, indicating that the presence of uranium inhibits the enzyme activity. This inhibitory effect can be, however, suppressed by an excess of calcium.

## Introduction

The incorporation of radioactive heavy metals, such as uranium (U), potentially represents a serious health risk to humans due to their chemo- and radiotoxicity. Uranium is ubiquitous in the environment, and can be found in the atmosphere, terrestrial and aquatic environments.<sup>1,2</sup> Ground- and surface waters, as well as soils, contain a trace amount of uranium originating from different sources such as mining activities,<sup>1,2</sup> the weathering of uranium-containing minerals,<sup>3-5</sup> the excessive use of phosphate fertilizers,<sup>5,6</sup> uranium-containing ammunition<sup>7,8</sup> or nuclear accidents.<sup>9,10</sup> According to the international standards for drinking water recommended by the World Health Organization (WHO),<sup>11-13</sup> the maximum contaminant level (MCL) for uranium is 30 µg/L (0.13 µM). The uranium concentrations in the majority of the contaminated drinking water are reported to be well below this MCL value.<sup>5,8,14</sup> However, there are also some cases reporting the uranium concentration of up to 1 mg/L (4.2 µM),<sup>3,14,15</sup> far exceeding the MCL value. These water sources and soils contaminated with uranium could eventually let uranium enter the human food chain. The human daily intake of uranium via drinking water and food is affected by the geological origin of the water sources and soils, varying from about 1 up to more than 200 µg/day.<sup>3-5</sup> In case of ingestion, more than 95% of uranium is excreted within a few days,<sup>5,16</sup> while the rest is distributed via the bloodstream throughout the body and finally deposited mainly in bone and kidney.<sup>1,5,16,17</sup> For this reason, the major concern about the uranium toxicity focuses on the damage primarily on kidney.<sup>3,15,18-20</sup> Additionally, it is known that uranium is genotoxic and carcinogenic.<sup>1,2,5</sup>

A series of our recent studies reporting the *in vitro* chemical speciation of radioactive actinides, such as uranium(VI) (as the uranyl ion,  $\text{UO}_2^{2+}$ ) or curium ( $\text{Cm}^{3+}$ ), in various body fluids (saliva, gastrointestinal fluids, urine and sweat) have suggested that organic biomolecules play a significant role in determining the chemical behavior of these radioactive

heavy metal ions in the body fluids.<sup>21-25</sup> These studies also revealed that bio-macromolecules, such as proteins or enzymes, could be the potential binding partners for the actinides under physiologically relevant conditions. These results indicate that (i) the proteins could support the uptake of the radionuclides into the body, and (ii) the structure and function of the proteins could be modified and/or affected via the interaction with the radionuclides. In order to perform a reliable assessment of the potential implication of the uptake of these radionuclides into human body, it is prerequisite to understand their chemical behavior with the bio-macromolecules being present in body fluids.

In the last decades, the studies on the chemical behavior of  $\text{UO}_2^{2+}$  in body fluids have focused primarily on the blood media to understand its interaction with the blood proteins (e.g., transferrin and albumin) that are mainly responsible for the transport of  $\text{UO}_2^{2+}$  through the body to the target organs in case of accidental incorporation.<sup>26-37</sup> On the other hand, there are only a limited number of studies reporting the chemical behavior of  $\text{UO}_2^{2+}$  in the gastrointestinal media as well as its interaction with digestive proteins.<sup>17,23,38</sup> Our recent investigation on the chemical speciation of  $\text{UO}_2^{2+}$  in saliva has suggested a strong interaction between  $\text{UO}_2^{2+}$  and the enzyme  $\alpha$ -amylase.<sup>23</sup> This motivated us to perform the present study focusing on the coordination and complexation behavior of  $\text{UO}_2^{2+}$  with  $\alpha$ -amylase, which is fundamental to understanding the implication of uranium uptake, particularly via oral ingestion, for human body.

The protein  $\alpha$ -amylase ( $\alpha$ -1,4-glucan-4-glucanhydrolase; EC 3.2.1.1.) is one of the major enzymes in salivary and pancreatic secretions of mammals. The protein catalyzes the hydrolysis of the  $\alpha$ -1,4-glycosidic linkages of polysaccharides, such as starch or glycogen.<sup>39</sup> The protein  $\alpha$ -amylase in human salivary and pancreatic juices, as well as in the porcine pancreatic juice, shows significant similarities in sequence and three-dimensional structure.<sup>40,41</sup> They consist of 496 amino acid residues with a molecular mass of ~55 kDa. The protein attaches one calcium and one chloride ions per molecule. It provides 50 carboxyl

groups from aspartic acid (Asp) and glutamic acid (Glu) side chains,<sup>42,43</sup> which potentially act as binding sites to interact with metal ions, such as  $\text{UO}_2^{2+}$ . The presence of calcium would be required to maintain the enzyme activity as well as to stabilize the structure of the protein.<sup>41</sup>

We herein report a comprehensive study on the complexation of  $\text{UO}_2^{2+}$  with  $\alpha$ -amylase under different conditions including physiologically relevant conditions, as well as its implication for the enzyme activity of  $\alpha$ -amylase. Batch sorption and potentiometric titration experiments were performed to investigate the macroscopic sorption and complexation behavior of  $\text{UO}_2^{2+}$  in the presence of  $\alpha$ -amylase. Time-resolved laser-induced fluorescence spectroscopy (TRLFS) and extended X-ray absorption fine structure (EXAFS) spectroscopy were carried out to acquire speciation information on possible  $\text{UO}_2^{2+}$   $\alpha$ -amylase species both in solution and in the solid state. Furthermore, the influence of  $\text{UO}_2^{2+}$  on the enzyme activity of  $\alpha$ -amylase was investigated *in vitro*.

## Materials and methods

### *Sorption experiments*

Batch sorption experiments were performed to investigate the affinity of  $\text{UO}_2^{2+}$  onto solid-state  $\alpha$ -amylase (porcine pancreatic  $\alpha$ -amylase, lyophilized powder supplied from Sigma). Although the macroscopic interaction of  $\text{UO}_2^{2+}$  with solid-state  $\alpha$ -amylase could be different from that with soluble  $\alpha$ -amylase, the sorption experiments give a macroscopic insight into the interaction between  $\text{UO}_2^{2+}$  and  $\alpha$ -amylase, providing supplementary information to understand the microscopic interaction of  $\text{UO}_2^{2+}$  with soluble  $\alpha$ -amylase. The experiments were carried out at room temperature and ambient conditions as functions of pH, metal- and enzyme concentrations, and sorption duration. The pH value was varied between 2.0 and 8.0 to cover physiological conditions of the gastrointestinal tract.<sup>44</sup> The  $\text{UO}_2^{2+}$  and  $\alpha$ -amylase concentrations were varied between  $10^{-6}$  and  $10^{-4}$  M and between 0.2 and 3.0 g/L ( $3.6 \times 10^{-6}$

to  $5.5 \times 10^{-5}$  M), respectively. The solubility of  $\alpha$ -amylase is below 0.1 g/L in the relevant conditions, confirming that  $\alpha$ -amylase exists as a solid phase during the experiments. The ionic strength was kept constant at 0.1 M with NaCl for all the experiments.

A stock solution of  $\text{UO}_2^{2+}$  was prepared by dissolving  $\text{UO}_2(\text{ClO}_4)_2 \cdot 6\text{H}_2\text{O}$  (p.a. from Merck) in a 0.1 M NaCl solution to give the desired  $\text{UO}_2^{2+}$  concentration. The pH value of the solution was then adjusted with HCl or NaOH. Subsequently,  $\alpha$ -amylase was added to the solution and the pH was adjusted again, if necessary. For pH- and concentration-dependent experiments, the mixture was shaken for 24 h at ambient temperature and the pH was adjusted after shaking as necessary. The solution was then centrifuged for 20 min at 4000 rpm and filtrated with a 150  $\mu\text{m}$  membrane filter. The pH value of the filtrate was measured and the uranium concentration was determined by inductively coupled plasma mass spectrometry (ICP-MS ELAN 9000 from Perkin-Elmer). Time-dependent experiments were performed at pH = 6.0, based on the results of the pH-dependent experiments. Fractions of the sample solution were collected at 2-min intervals for the first 10 min, and then at 5-min intervals until 60 min. The collected fractions were filtrated with a 150  $\mu\text{m}$  membrane filter, and the uranium concentration in the filtrate was determined with ICP-MS.

The data from the batch sorption experiments at a constant pH were fitted using the Hill equation (Eq. 1)<sup>45</sup> with OriginPro9.0 (OriginLab, USA) to estimate the number of binding sites ( $g$ ), the association equilibrium constant ( $K_H$ ) and the Hill coefficient ( $r$ ) based on the experimentally determined saturation function,  $v$ , with the unit of “bound  $\text{UO}_2^{2+}$  (mol) /  $\alpha$ -amylase (mol)”, and the free  $\text{UO}_2^{2+}$  concentration ( $[\text{UO}_2^{2+}]$ );

$$v = \frac{g(K_H[\text{UO}_2^{2+}])^r}{1 + (K_H[\text{UO}_2^{2+}])^r} \quad (1).$$



### ***Potentiometric titration***

Potentiometric titration experiments were performed to determine the stability constants for the  $\text{UO}_2^{2+}$ - $\alpha$ -amylase complexes. All sample preparation and measurements were carried out under  $\text{N}_2$  atmosphere to prevent the possible formation of  $\text{UO}_2^{2+}$ -carbonate species. 3 mg of  $\alpha$ -amylase was dissolved in 30 mL of deionized carbonate-free  $\text{H}_2\text{O}$ . The protein concentration in the resultant solution was 0.1 g/L ( $1.8 \times 10^{-6}$  M), which is equivalent to  $9 \times 10^{-5}$  M carboxyl groups by assuming that one  $\alpha$ -amylase provides 50 carboxyl side chains from Asp and Glu.<sup>42,43</sup> The  $\text{UO}_2^{2+}$  stock solution was then added to give a final uranium concentration of  $10^{-4}$  M. Subsequently, the ionic strength of the solution was adjusted to 0.1 M with NaCl, and the pH value was adjusted at 3 with HCl. The sample solution was automatically titrated in a thermostatic vessel at  $25.0 \pm 0.1$  °C with 736 GP Titrino/TiNet 2.50 (Metrohm) with 0.1 M NaOH (carbonate-free, Titrisol, Merck). Dynamic titration was performed using a BlueLine11 electrode (Schott) with a minimum drift of 0.5 mV/min and a delay time of at least 60 s at each pH measurement. Prior to each titration experiment, the electrode was calibrated with standard buffers of pH = 4.008, 6.865 and 9.180 (Schott). The experiments were carried out in triplicate in the pH range between 3 and 7 in order to guarantee the absence of precipitation of uranyl hydroxides.

In order to take into account the nature and concentration of functional groups of the protein on the calculation of the complex formation constants ( $\beta_{\text{ML}}$ ), the following equations were applied:



where  $\text{M}^{2+}$  is  $\text{UO}_2^{2+}$ , R-LH is the protein Amy with the dissociable functional groups LH ( $-\text{COOH}$ ,  $-\text{NH}_3^+$ , and  $-\text{OH}$ ) and  $x = 1$  or 2. The data from the potentiometric titration were

treated using the program HYPERQUAD2008 (Protonic Software)<sup>46</sup> to obtain the  $\log \beta$  values. The deprotonation constants of  $\alpha$ -amylase ( $pK_a = -\log K_a$ ) have been determined recently.<sup>47</sup> The values of  $pK_{a1} = 5.23$  for carboxyl groups and  $pK_{a2} = 10.22$  for amino and/or hydroxyl groups were considered in the calculations of stability constants. The latest stability constants provided by the Nuclear Energy Agency – Thermodynamical Database (NEA-TDB)<sup>48</sup> were employed for aqueous uranyl(VI) hydroxyl complexes. The obtained  $\log \beta$  values were extrapolated to infinite dilution by applying the Specific Interaction Theory (SIT) using the IUPAC software for Ionic Strength Corrections.<sup>49</sup> Distribution of  $UO_2^{2+}$  species was calculated using the computer programs HYDRA and MEDUSA.<sup>50</sup>

### ***Time-resolved laser-induced fluorescence spectroscopy***

Time-resolved laser-induced fluorescence spectroscopy (TRLFS) measurements were performed to acquire information about the  $UO_2^{2+}$ - $\alpha$ -amylase species formed in solution. The uranium and protein concentrations in the sample solutions were fixed at  $1 \times 10^{-5}$  M and 0.1 g/L ( $1.8 \times 10^{-6}$  M  $\alpha$ -amylase resp.  $9 \times 10^{-5}$  M carboxyl groups), respectively. The measurements were carried out as a function of pH between 2.0 and 8.0, equivalent to the sorption experiments. The samples were prepared in a glove box filled with  $N_2$  to prevent the possible formation of  $UO_2^{2+}$ -carbonate species. The ionic strength was kept constant at 0.1 M with a  $NaClO_4$  stock solution. The pH adjustments were carried out with a BlueLine 16 pH electrode (Schott) using  $HClO_4$  or  $NaOH$  as necessary. The sample solutions were equilibrated for 24 h prior to the measurements. The spectra were recorded at  $25 \pm 1$  °C using a pulsed Nd:YAG laser system (Continuum Minilite Electro-Optics, Inc., Santa Clara, USA) with a fast pulse generator (FPG/05, EG&G Princeton Instruments, NJ, USA) and a digital delay generator (Uniblitz, model VVM-D1, Vincent Associates, NY). The excitation wavelength of the uranyl fluorescence was 266 nm with pulse energy of 0.2 - 0.5 mJ. The spectra were collected with a diffraction grating of  $100 \text{ mm}^{-1}$  from 371 to 674 nm and a gate

width of 2  $\mu$ s. Three spectra recorded with 200 laser shots were averaged. The fluorescence emission was monitored using an iHR 550 spectrograph (Horiba Jobin Yvon, Germany) with the software LabSpec5 (Horiba Jobin Yvon, Germany). For the time-resolved measurements, 40 to 60 spectra were collected over a delay time range of 0.1 to 100  $\mu$ s with delay time intervals between 0.5 and 10  $\mu$ s.

The collected TRLFS data were analyzed with OriginPro9.0. The lifetimes of luminescent species were determined according to the following equation:

$$E(t) = \sum_i E_i \times \exp(-t/\tau_i) \quad (4),$$

where  $E$  is the total luminescence intensity at the time  $t$ ,  $E_i$  is the luminescence intensity of the species  $i$  at  $t = 0$ , and  $\tau_i$  is the corresponding lifetime. The static spectra were analyzed using the program SPECFIT<sup>51</sup> to calculate the spectra of individual species.

### ***Extended X-ray absorption fine structure spectroscopy***

Extended X-ray absorption fine structure (EXAFS) spectroscopy was performed at U  $L_{III}$ -edge to obtain structural information of  $UO_2^{2+}$  bound to  $\alpha$ -amylase. 200 mg of solid  $\alpha$ -amylase were added to 18 mL of 1 mM  $UO_2^{2+}$  solution, resulting in 3.5  $\mu$ mol  $\alpha$ -amylase and 18  $\mu$ mol of  $UO_2^{2+}$  in the resultant suspensions. The pH was then adjusted to 3.5 or 6.0. The suspensions were then shaken for 3 h and centrifuged for 20 min at 4000 rpm. The uranium concentration in the centrifuge effluent was determined with ICP-MS, confirming that ~95 % of the initial  $UO_2^{2+}$  was sorbed on  $\alpha$ -amylase for the both samples. This indicates a  $UO_2^{2+}$  :  $\alpha$ -amylase stoichiometry of 5 : 1 in the samples, which is equivalent to a  $UO_2^{2+}$  : carboxyl stoichiometry of 1 : 10.

The solid phases obtained after centrifugation were sealed in a Teflon sample holder as wet paste, shock-frozen and stored in liquid nitrogen until immediately before the EXAFS

measurements. EXAFS measurements were carried out at the Rossendorf Beamline<sup>52</sup> at the European Synchrotron Radiation Facility (ESRF). The U  $L_{III}$ -edge X-ray absorption spectra were measured in a fluorescence mode with a 13-element germanium detector (Canberra). The spectra were collected at 15 K using a closed cycle helium cryostat. Eight spectra were recorded for each sample and averaged for data analysis. For energy calibration of the collected spectra, the  $K$ -edge X-ray absorption spectrum of yttrium foil (17038 eV) was recorded simultaneously. The U  $L_{III}$ -edge ionization potential was tentatively defined as 17185 eV and refined during the fitting routine. The EXAFS spectra were analyzed according to standard procedures including statistical weighting of the 13 fluorescence channels and dead-time correction using EXAFSPAK.<sup>53</sup> Theoretical phase and amplitude functions were calculated with the software FEFF 8.2<sup>54</sup> based on the crystal structure of sodium uranyl(VI) triacetate,  $\text{NaUO}_2(\text{CH}_3\text{COO})_3$ ,<sup>55</sup> and uranyl(VI)dibromo-bis( $N,N$ -bis(2-butyl)isobutyramide),  $\text{UO}_2\text{Br}_2[\text{C}_3\text{H}_7\text{C}(\text{O})\text{N}(\text{C}_4\text{H}_9)_2]_2$ ,<sup>56</sup> for carboxyl- and carbonyl units, respectively.

### ***Enzyme activity measurements***

The influence of  $\text{UO}_2^{2+}$  on the enzyme activity of  $\alpha$ -amylase was investigated according to the method by Bernfeld.<sup>57</sup> The enzyme assay was prepared as follows: (i) a 1 mL of 1 % (w/v) starch solution (in Tris buffer) was mixed with a 1 mL of 0.1 % (w/v) enzyme solution and the resultant solution was stirred for 3 min, (ii) a 1 mL of a color reagent (96 mM of 3,5-dinitrosalicylic acid in tartrate/NaOH solution) was added to the solution, capped, placed in a boiling water bath for 15 min, and cooled down to room temperature on ice, and (iii) after the addition of 9 mL of deionized water, the absorption at 540 nm was recorded. The blank was prepared in the same manner without enzyme. To investigate the effect of  $\text{UO}_2^{2+}$  on the enzyme activity, the enzyme solution was spiked either with  $\text{UO}_2^{2+}$  or a mixture of  $\text{UO}_2^{2+}$  and  $\text{Ca}^{2+}$  ( $[\text{UO}_2^{2+}]_{\text{total}} = 10^{-7} - 10^{-4}$  M and  $[\text{Ca}^{2+}]_{\text{total}} = 10^{-3}$  M). The enzyme activity without metal ions was set as 100 %.

## Results and discussion

### *Affinity of uranium for $\alpha$ -amylase*

Batch sorption experiments were performed to acquire a macroscopic overview of the interaction behavior of  $\text{UO}_2^{2+}$  with  $\alpha$ -amylase. The affinity of  $\text{UO}_2^{2+}$  for  $\alpha$ -amylase as a function of pH with three different uranium concentrations is shown in Figure 1-left. Regardless of the uranium concentration, the sorption of  $\text{UO}_2^{2+}$  begins at around pH 2.5, approaches more than 90 % of sorption at pH 4.5, and then reaches a plateau above pH 4.5. When the pH further increases above pH 6, the sorption decreases slightly. This behavior could be caused by the formation of highly soluble uranyl carbonate species,<sup>58</sup> which probably originates from the absorption of residuals of  $\text{CO}_2$  from air in the sample solution. Based on these results, the pH value for the following batch experiments was set between 5 and 6, where the sorption of  $\text{UO}_2^{2+}$  reaches ~95 %. It has been reported that  $\alpha$ -amylase keeps the maximum enzyme activity in the range between pH = 5.5 and 8.0,<sup>41</sup> suggesting that  $\alpha$ -amylase keeps the highest enzyme activity under the current experimental conditions between pH 5 and 6.

The time-dependent sorption behavior of  $\text{UO}_2^{2+}$  with two different  $\alpha$ -amylase concentrations is shown in Figure 1-right. The sorption of  $\text{UO}_2^{2+}$  begins within the first few minutes and reaches a plateau after 5 min. This time frame could be relevant to the contact time of substances with saliva in the mouth, where the retention time of the ingested food could last up to several minutes.<sup>44</sup> Moreover,  $\alpha$ -amylase can be also found in pancreatic juice,<sup>40,41</sup> indicating that this time frame is of particular relevance to the gastrointestinal tract, where the retention time is much longer (up to several hours).<sup>44</sup> Under the same conditions,  $\text{Eu}^{3+}$  was sorbed only ~30 and 60 % at 0.5 and 1.0 g/L of  $\alpha$ -amylase concentrations, respectively,<sup>47</sup>

while  $\text{UO}_2^{2+}$  was sorbed ~70 and 90 %, respectively (see Figure 1-right). This suggests a higher affinity of  $\text{UO}_2^{2+}$  for  $\alpha$ -amylase than that of  $\text{Eu}^{3+}$ .

Figure 2 shows the binding isotherm of  $\alpha$ -amylase as a function of uranium concentration. By fitting the experimental data with the Hill equation (Eq. 1),<sup>45</sup> which is a modification of the Langmuir sorption isotherm, we can obtain the information about the macroscopic interaction between  $\text{UO}_2^{2+}$  and enzyme. The term  $r$  in Eq. 1 is the Hill coefficient, where “ $r = 1$ ” stands for non-cooperative systems (*i.e.*, identical or non-identical independent binding sites), “ $r > 1$ ” for positively, and “ $r < 1$ ” for negatively cooperative systems (*i.e.*, interacting binding sites). Based on the data in Figure 2, the  $r$  value was calculated to be  $1.5 \pm 0.3$  with  $g = 19 \pm 2$ , suggesting that  $\alpha$ -amylase provides approximately 19 binding sites to  $\text{UO}_2^{2+}$  with a weakly positive cooperative character. The corresponding association constant for  $\text{UO}_2^{2+}$ , which represents an average value for all the possible binding sites of  $\alpha$ -amylase, was calculated to be  $\log K_H = 5.0 \pm 0.1$ . The  $r$  value for  $\text{Eu}^{3+}$  was calculated to be  $1.1 \pm 0.2$  (*i.e.*, nearly non-cooperative system) with 3 binding sites, and the corresponding association constant was  $\log K_H = 6.4 \pm 0.1$ ,<sup>47</sup> which is significantly larger than that of  $\text{UO}_2^{2+}$ . However,  $\text{Eu}^{3+}$  is assumed to replace the  $\text{Ca}^{2+}$  at the specific binding site on  $\alpha$ -amylase.<sup>47</sup> Given this fact, the larger number of binding sites for  $\text{UO}_2^{2+}$  indicates that the sorption of  $\text{UO}_2^{2+}$  on  $\alpha$ -amylase occurs unspecifically at any possible binding sites, which is different from the specific sorption of  $\text{Eu}^{3+}$ . This difference in sorption behavior could also explain the difference in association constants between  $\text{UO}_2^{2+}$  and  $\text{Eu}^{3+}$ . Furthermore, the weak positive cooperative character of association for  $\text{UO}_2^{2+}$  could also indicate that the  $\text{UO}_2^{2+}$  binds onto the surface of the protein and subsequently induces the alteration of protein structure (opening or unfolding), providing additional coordination sites for the sorbed  $\text{UO}_2^{2+}$ . In fact, this effect was observed for the interaction of  $\text{UO}_2^{2+}$  with hemoglobin and human serum albumin,<sup>36,37</sup> where the  $\text{UO}_2^{2+}$  alters the secondary conformation of these proteins and, as a result, significantly decreases the  $\alpha$ -helix structures.<sup>36,37</sup>

### ***Potentiometric titration***

Potentiometric titration was carried out to gain a further insight into the solution chemistry associated with the interaction between  $\text{UO}_2^{2+}$  and  $\alpha$ -amylase. With potentiometric pH titration measurements, the functional groups of  $\alpha$ -amylase with exchangeable protons can be identified based on Eqs. (2) and (3), that is, carboxyl- ( $\text{R-COOH} \rightleftharpoons \text{R-COO}^- + \text{H}^+$ ), hydroxyl- ( $\text{R-OH} \rightleftharpoons \text{R-O}^- + \text{H}^+$ ) and amino ( $\text{R-NH}_3^+ \rightleftharpoons \text{R-NH}_2 + \text{H}^+$ ) groups.  $\alpha$ -amylase provides a wide variety of functional groups for the interaction with metal ions. In addition to the carboxyl groups from Asp and Glu residues, the phenol groups from tyrosine (Tyr), the hydroxyl groups from serine (Ser) and threonine (Thr), and the amino groups from arginine (Arg), asparagine (Asn), glutamine (Gln), and lysine (Lys) are the potential binding sites for metal ions. The deprotonation constants ( $\text{p}K_a$ ) of these functional groups have been recently determined.<sup>47</sup> Based on Eqs. (2) and (3) together with the reported  $\text{p}K_a$  values listed in Table 1, four different complexes were identified under the current experimental conditions. In the slightly acidic region of  $\text{pH} = 3\sim 6$ , the complex with a  $\text{UO}_2^{2+} : \alpha$ -amylase stoichiometry of 1 : 1 via the carboxylic groups of  $\alpha$ -amylase,  $\text{UO}_2(\text{R-COO})^+$ , is formed. With increasing pH, similar complexes with one- and two hydroxo groups,  $\text{UO}_2\text{OH}(\text{R-COO})$  and  $\text{UO}_2(\text{OH})_2(\text{R-COO})^-$ , become major species up to the slightly basic pH of 8. The relevant stability constants considering the interaction via a single carboxylic group of  $\alpha$ -amylase were determined to be  $\log \beta_{110} = 5.67 \pm 0.08$  for  $\text{UO}_2(\text{R-COO})^+$ ,  $\log \beta_{11-1} = 0.64 \pm 0.07$  for  $\text{UO}_2\text{OH}(\text{R-COO})$ , and  $\log \beta_{11-2} = -6.29 \pm 0.17$  for  $\text{UO}_2(\text{OH})_2(\text{R-COO})^-$ . The results also indicate the formation of another complex with two carboxylic groups from the identical or different  $\alpha$ -amylase molecule(s) interacting with  $\text{UO}_2^{2+}$ ,  $\text{UO}_2(\text{R-COO})_2$ , in the pH range between 4 and 6 (Figure 3-left). The relevant stability constant was calculated to be  $\log \beta_{120} = 10.39 \pm 0.21$ . All the identified complexes and relevant stability constants are summarized in Table 1.

### *Time-resolved laser-induced fluorescence spectroscopy*

TRLFS measurements were performed to further investigate the solution speciation of the  $\text{UO}_2^{2+}$ - $\alpha$ -amylase complexes. The luminescence spectra of  $\text{UO}_2^{2+}$  in the aqueous solution containing  $\alpha$ -amylase at different pH values are given in Figure 4. In the pH range between 2 and 8, the peak maxima of the spectra showed a red shift as compared to that for the pure aquo species of  $\text{UO}_2^{2+}$  ion (black data in Figure 4). The luminescence intensity increased when the pH increased from 2 to 3, which is much stronger than that for the pure aquo species of  $\text{UO}_2^{2+}$  ion (Figure 4-a). When the pH increased from pH 3 to 6, the intensity further decreased. No further change was observed above pH = 6 up to 8 (Figure 4-b and c). The time-resolved luminescence spectra indicate two independent luminescence lifetimes of  $t_1 = 7.1 \pm 1.3 \mu\text{s}$  and  $t_2 = 22.1 \pm 2.3 \mu\text{s}$ , both of which are different from that of either the pure aquo species of  $\text{UO}_2^{2+}$  ion or uranyl hydroxyl complexes (Table 2).<sup>59-62</sup> This suggests that at least two independent luminescent species can be considered for the  $\text{UO}_2^{2+}$  ion interacting with the protein  $\alpha$ -amylase. On the other hand, the species distribution derived from the potentiometric titration experiments (Figure 3-right) shows the formation of four different  $\text{UO}_2^{2+}$ - $\alpha$ -amylase complexes in the pH range between 2 and 8. Given these facts, one could interpret the observed decrease of luminescence intensity at the higher pH range as the formation of non-luminescence  $\text{UO}_2^{2+}$  species most likely affected by strong quenching processes at least at room temperature. Such a quenching effect at room temperature has been observed for the  $\text{UO}_2^{2+}$  ions interacting with several organic ligands.<sup>59,63-68</sup>

Using the complex stability constants determined by potentiometric titration (Table 1), we further analyzed the TRLF spectra with the factor analysis program SPECFIT.<sup>51</sup> The factor analysis of the static spectra resulted in two independent spectra, indicating the presence of two luminescent  $\text{UO}_2^{2+}$ - $\alpha$ -amylase species. The resultant two spectra could be assigned to the species  $\text{UO}_2(\text{R-COO})^+$  and  $\text{UO}_2(\text{R-COO})_2$  (Figure 5), whereas the other hydroxyl containing species derived from the speciation calculation (Figure 3), that is  $\text{UO}_2\text{OH}(\text{R-COO})$  and



$\text{UO}_2(\text{OH})_2(\text{R-COO})^-$ , are likely to be the non-luminescent species. Although the latter hydroxyl containing species are supposed to be non-luminescent, their inclusion on the factor analysis is required to obtain reasonable deconvolution results, supporting the possible formation of these species in the sample solutions.

Based on the change of luminescence spectra as a function of pH (Figure 4) and the speciation distribution (Figure 3), the observed longer lifetime dominating at lower pH can be assigned to the species  $\text{UO}_2(\text{R-COO})^+$ , while the shorter one dominating at higher pH can be assigned to the species  $\text{UO}_2(\text{R-COO})_2$  (Table 2).

### ***Extended X-ray absorption fine structure spectroscopy***

EXAFS spectroscopy was employed to acquire information about the local structure arrangement around  $\text{UO}_2^{2+}$  when it is sorbed on  $\alpha$ -amylase. Figure 6 shows the  $k^3$ -weighted U  $L_{\text{III}}$ -edge EXAFS spectra for  $\text{UO}_2^{2+}$  sorbed on  $\alpha$ -amylase at two different pH values and their corresponding Fourier transforms (FTs). The EXAFS structural parameters obtained from theoretical fitting are summarized in Table 3. The interatomic distances ( $R$ ) of 1.78-1.79 Å calculated for U- $\text{O}_{\text{ax}}$  are typical of the uranyl(VI) arrangement (i.e.  $\text{UO}_2^{2+}$ ) and also found for the uranyl(VI) complexes sorbed on biological substances.<sup>33,34,69-72</sup>

The second largest FT peaks at around  $R + \Delta = 1.9$  Å in Figure 6-right can be interpreted as the scattering from two different oxygen shells in the equatorial plane of  $\text{UO}_2^{2+}$ . The shorter U- $\text{O}_{\text{eq}}$  distances (U- $\text{O}_{\text{eq1}} = 2.30$  and 2.33 Å in Table 3) are significantly longer than those for typical U-OH distances (2.24 Å),<sup>73</sup> but also shorter than those for typical U- $\text{H}_2\text{O}$  distances (2.41 Å).<sup>73</sup> The longer U- $\text{O}_{\text{eq}}$  distances (U- $\text{O}_{\text{eq2}} = 2.48$  and 2.52 Å in Table 3) are significantly longer than those for the typical U- $\text{H}_2\text{O}$  distances as well. This indicates that the coordination environment around the  $\text{UO}_2^{2+}$  ions sorbed on the protein is significantly different from that of either hydroxo- or aquo species of  $\text{UO}_2^{2+}$  ions. The shorter U- $\text{O}_{\text{eq}}$  distances (U- $\text{O}_{\text{eq1}} = 2.30$  and 2.33 Å at pH 3.5 and 6.0, respectively) are comparable with the U-O distances observed

for monodentately coordinating carboxylic groups in small organic molecules and peptides (2.25 – 2.32 Å).<sup>74-77</sup> The Asp and Glu groups in  $\alpha$ -amylase, but also the carbonyl moieties (*i.e.* amide) of the peptide main chain and/or the side chains of Asn and Gln, and the phenolic units from Tyr can be considered for such shorter U-O distances.<sup>75,78-80</sup> On the other hand, the longer U-O<sub>eq</sub> distances (U-O<sub>eq2</sub> = 2.48 and 2.52 Å at pH = 3.5 and 6.0, respectively) are in good agreement with a typical U-O<sub>eq</sub> distance for bidentately coordinating carboxylate groups (2.45 – 2.49 Å).<sup>74-77,81</sup> Additionally, the FT peaks appeared at around  $R + \Delta = 2.2$  Å in Figure 6-right can be interpreted as the single scattering from the C atoms of bidentately coordinating carboxylate groups. In fact, the calculated interatomic distances of 2.84 and 2.93 Å are in the range of the typical U-C distance for bidentately coordinating carboxylate ligands (2.88 – 2.93 Å).<sup>74-76,81</sup> Given these facts, it is reasonable to conclude that the UO<sub>2</sub><sup>2+</sup> ions sorbed on  $\alpha$ -amylase are primarily surrounded by 3-4 carboxyl/ate groups both in mono- and bidentate binding modes. However, possible coordination with carbonyl- or phenolate groups are also reported,<sup>75,78-80</sup> and its possibility cannot be completely excluded. The lengthening of U-O<sub>eq</sub> distances with increasing pH (from 3.5 to 6.0, Table 3) can be attributed to the rearrangement of coordinating carboxyl/ate groups from mono- to bidentate modes that is induced by the deprotonation of carboxyl groups. In fact, the structural parameters obtained from EXAFS theoretical fitting are the average of major species present in the sample and are less sensitive for minor species.

### ***Enzyme activity study***

The results discussed above indicate a significant interaction between UO<sub>2</sub><sup>2+</sup> and  $\alpha$ -amylase, one of the major enzymes in saliva. Since this interaction has been proven to be significant even in the actual salivary media,<sup>23</sup> the effect of UO<sub>2</sub><sup>2+</sup> on the enzyme activity of  $\alpha$ -amylase was further investigated.

Shown in Figure 7 are the relative activities of  $\alpha$ -amylase as a function of uranium concentration without- and with an excess of  $\text{Ca}^{2+}$ . The enzyme activity decreases significantly with increasing the uranium concentration. Lower uranium concentrations of  $10^{-7}$  M and  $10^{-6}$  M do not affect the enzyme activity. However, rising the uranium concentration to  $10^{-5}$  M results in the reduction of enzyme activity to ~60 %, which is further reduced down to ~30 % when the uranium concentration rises to  $10^{-4}$  M. The enzyme activity is completely restrained when the uranium concentration reaches  $10^{-3}$  M. These results are in accordance with the precedent study by Schneyer, reporting the inhibition of the enzyme activity of  $\alpha$ -amylase by  $\text{UO}_2^{2+}$ .<sup>82</sup> This precedent study also indicated that the inhibition effect by  $\text{UO}_2^{2+}$  is reversible, and the addition of  $\alpha$ -hydroxo-dicarboxylic acids, such as citrate or malate, after the inhibition phenomenon results in the reactivation of the enzyme activity. This reactivation phenomenon was interpreted as a result of the preferable complexation of  $\text{UO}_2^{2+}$  with the small organic acids (i.e. citrate or malate) that have stronger coordination ability than  $\alpha$ -amylase.<sup>82</sup>

When an excess of  $\text{Ca}^{2+}$  ( $[\text{Ca}^{2+}]_{\text{total}} = 10^{-3}$  M) was added to the system containing  $\text{UO}_2^{2+}$ , the inhibiting effect of  $\text{UO}_2^{2+}$  was not only compensated, but also the enzyme activity was rather increased slightly (Figure 7). The effect of  $\text{Ca}^{2+}$  to suppress the inhibition effect of  $\text{UO}_2^{2+}$  could be interpreted as follows. First,  $\text{Ca}^{2+}$  occupies the binding sites on  $\alpha$ -amylase more dominantly and/or faster than  $\text{UO}_2^{2+}$  that is attached to the binding sites of  $\alpha$ -amylase unspecifically, eventually preventing  $\text{UO}_2^{2+}$  from the binding on  $\alpha$ -amylase. A similar phenomenon was also observed for the interaction of  $\text{Eu}^{3+}$  with  $\alpha$ -amylase.<sup>47</sup> However, the sorption of  $\text{Eu}^{3+}$  occurs on specific binding sites of  $\alpha$ -amylase<sup>47</sup> and, therefore, its sorption mechanism is different from that of  $\text{UO}_2^{2+}$ . Second, the soluble and stable  $\text{Ca}_2\text{UO}_2(\text{CO}_3)_3(\text{aq})$  complex<sup>83</sup> at higher pH is formed due to the absorption of residual  $\text{CO}_2$  from air in the sample solution, which overcomes the binding of  $\text{UO}_2^{2+}$  onto  $\alpha$ -amylase. Both the effects could complement each other. The enhancement of  $\alpha$ -amylase activity by  $\text{Ca}^{2+}$  could be caused by

the stabilization of enzyme conformation by  $\text{Ca}^{2+}$  ions interacting with Asp and Glu residues.<sup>41</sup> The concentration of  $\text{Ca}^{2+}$  employed in these experiments is relevant to the average concentration in the gastrointestinal tract, which contains the enzyme  $\alpha$ -amylase from saliva and pancreatic juice.<sup>21,23</sup> This suggests that the actual amount of  $\text{Ca}^{2+}$  in the body fluids could be sufficient to suppress the effect of  $\text{UO}_2^{2+}$  on the digestive function of the enzyme  $\alpha$ -amylase.

## Conclusions

We investigated the interaction of  $\text{UO}_2^{2+}$  with the digestive enzyme  $\alpha$ -amylase over a pH range of 2-8 and uranium/  $\alpha$ -amylase concentrations with a suite of analytical methods. Batch sorption experiments showed a fast and strong interaction of  $\text{UO}_2^{2+}$  with  $\alpha$ -amylase over the pH range that is representative for the *in vivo* conditions of the human gastrointestinal tract, which is consistent with the results for the interaction of  $\text{Eu}^{3+}$  with  $\alpha$ -amylase.<sup>47</sup> Complex stability constants for four  $\text{UO}_2^{2+}$   $\alpha$ -amylase species were determined by assuming the interactions via the carboxyl functionality of  $\alpha$ -amylase. These constants contribute to the improvement of the relevant thermodynamic calculation by supplementing the lack of thermodynamic data on bio-macromolecules.<sup>21-23,84</sup> Although it is obvious that  $\alpha$ -amylase is an important enzyme that potentially affects the behavior of uranium in saliva and pancreatic juice, the interaction between uranium and  $\alpha$ -amylase in the actual human digestive system occurs in the presence of mucus and other glycoproteins (e.g., mucin, lactoferrin, immunoglobulins, etc.). It is therefore important to further investigate the competition of uranium coordination among  $\alpha$ -amylase and these glycoproteins, which is surely our future work. It was also confirmed that  $\text{UO}_2^{2+}$  could reduce the enzyme activity of  $\alpha$ -amylase. However, given the maximum acceptable level of uranium contamination recommended by the WHO ( $0.13 \mu\text{M}$ )<sup>11-13</sup> and the maximum acceptable intake of uranium via drinking water or

food (~200 µg/day),<sup>3-5</sup> the chemotoxic effect of uranium is not expected at least in terms of the enzyme activity of  $\alpha$ -amylase. Such a chemotoxic effect could be inhibited by an excess of  $\text{Ca}^{2+}$  that is relevant to physiological conditions, in any case. The chemotoxicity of uranium would be an issue primarily when a larger amount of uranium intake is expected by accidental releases, etc. The quantitative information obtained in this study could contribute to the reliable assessment of the health risk of uranium when incorporated into the human body.

## Acknowledgements

The authors thank Mrs. Ursula Schaefer for ICP-MS measurements and Mrs. Claudia Jähnigen for technical assistance with potentiometric titration experiments, sample preparation for TRLFS and enzyme activity studies.

## Abbreviations

EXAFS, extended X-ray absorption fine structure;  $I$ , ionic strength; ICP-MS, inductively coupled plasma mass spectrometry; IUPAC, International Union of Pure and Applied Chemistry;  $\log \beta$ , complex stability constant; Nd:YAG, neodymium-doped yttrium aluminum garnet; NEA-TDB, Nuclear Energy Agency – Thermodynamical Database; SIT, Specific Interaction Theory; TRLFS, time-resolved laser-induced fluorescence spectroscopy

## References

- (1) Brugge, D., and Buchner, V. (2011) Health effects of uranium: new research findings. *Rev. Environ. Health*, 26, 231-249.
- (2) Brugge, D., deLemos, J. L., and Oldmixon, B. (2005) Exposure Pathways and Health Effects Associated with Chemical and Radiological Toxicity of Natural Uranium: A Review. *Rev. Environ. Health*, 20, 177-193.

- (3) Kurttio, P., Auvinen, A., Salonen, L., Saha, H., Pekkanen, J., Makelainen, I., Vaisanen, S. B., Penttila, I. M., and Komulainen, H. (2002) Renal effects of uranium in drinking water. *Environ. Health Perspect.*, 110, 337-342.
- (4) Anke, M., Seeber, O., Müller, R., Schäfer, U., and Zerull, J. (2009) Uranium transfer in the food chain from soil to plants, animals and man. *Chem Erde-Geochem.*, 69, 75-90.
- (5) Bjorklund, G., Christophersen, O. A., Chirumbolo, S., Selinus, E., and Aaseth, J. (2017) Recent aspects of uranium toxicology in medical geology. *Environ. Res.*, 156, 526-533.
- (6) Schnug, E., and Lottermoser, B. G. (2013) Fertilizer-Derived Uranium and its Threat to Human Health. *Environ. Sci. Technol.*, 47, 2433-2434.
- (7) Handley-Sidhu, S., Keith-Roach, M. J., Lloyd, J. R., and Vaughan, D. J. (2010) A review of the environmental corrosion, fate and bioavailability of munitions grade depleted uranium. *Sci. Total Environ.*, 408, 5690-5700.
- (8) Berisha, F., and Goessler, W. (2013) Uranium in Kosovo's drinking water. *Chemosphere*, 93, 2165-2170.
- (9) Burns, P. C., Ewing, R. C., and Navrotsky, A. (2012) Nuclear Fuel in a Reactor Accident. *Science*, 335, 1184-1188.
- (10) Shinonaga, T., Steier, P., Lagos, M., and Ohkura, T. (2014) Airborne Plutonium and Non-Natural Uranium from the Fukushima DNPP Found at 120 km Distance a Few Days after Reactor Hydrogen Explosions. *Environ. Sci. Technol.*, 48, 3808-3814.
- (11) Ansoborlo, E., Lebaron-Jacobs, L., and Prat, O. (2015) Uranium in drinking-water: A unique case of guideline value increases and discrepancies between chemical and radiochemical guidelines. *Environ. Int.*, 77, 1-4.
- (12) WHO. (2011) Uranium in Drinking-water. Background document for development of WHO Guidelines for Drinking-water Quality. 29 pp.
- (13) WHO. (2011) Guidelines for Drinking-water Quality. 564 pp. Geneva.
- (14) Waseem, A., Ullah, H., Rauf, M. K., and Ahmad, I. (2015) Distribution of Natural Uranium in Surface and Groundwater Resources: A Review. *Crit. Rev. Environ. Sci. Technol.*, 45, 2391-2423.
- (15) Magdo, H. S., Forman, J., Graber, N., Newman, B., Klein, K., Satlin, L., Amler, R. W., Winston, J. A., and Landrigan, P. J. (2007) Grand rounds: Nephrotoxicity in a young child exposed to uranium from contaminated well water. *Environ. Health Perspect.*, 115, 1237-1241.

- (16) Konietzka, R. (2015) Gastrointestinal absorption of uranium compounds - A review. *Regul. Toxicol. Pharm.*, *71*, 125-133.
- (17) Ansoborlo, E., Prat, O., Moisy, P., Den Auwer, C., Guilbaud, P., Carriere, M., Gouget, B., Duffield, J., Doizi, D., Vercouter, T., Moulin, C., and Moulin, V. (2006) Actinide speciation in relation to biological processes. *Biochimie*, *88*, 1605-1618.
- (18) Selden, A. I., Lundholm, C., Edlund, B., Hogdahl, C., Ek, B. M., Bergstrom, B. E., and Ohlson, C. G. (2009) Nephrotoxicity of uranium in drinking water from private drilled wells. *Environ. Res.*, *109*, 486-494.
- (19) Zamora, M. L. L., Zielinski, J. M., Moodie, G. B., Falcomer, R. A. F., Hunt, W. C., and Capello, K. (2009) Uranium in Drinking Water: Renal Effects of Long-Term Ingestion by an Aboriginal Community. *Arch. Environ. Occup. Health*, *64*, 228-241.
- (20) Kurttio, P., Harmoinen, A., Saha, H., Salonen, L., Karpas, Z., Komulainen, H., and Auvinen, A. (2006) Kidney toxicity of ingested uranium from drinking water. *Am. J. Kidney Dis.*, *47*, 972-982.
- (21) Barkleit, A., Wilke, C., Heller, A., Stumpf, T., and Ikeda-Ohno, A. (2017) Trivalent f-elements in human saliva: A comprehensive speciation study by time-resolved laser-induced fluorescence spectroscopy and thermodynamic calculations. *Dalton Trans.*, *46*, 1593-1605.
- (22) Wilke, C., Barkleit, A., Stumpf, T., and Ikeda-Ohno, A. (2017) Speciation of the trivalent f-elements Eu(III) and Cm(III) in digestive media. *J. Inorg. Biochem.*, *175*, 248-258.
- (23) Osman, A. A. A., Geipel, G., Barkleit, A., and Bernhard, G. (2015) Uranium(VI) Binding Forms in Selected Human Body Fluids: Thermodynamic Calculations versus Spectroscopic Measurements. *Chem. Res. Toxicol.*, *28*, 238-247.
- (24) Heller, A., Barkleit, A., Foerstendorf, H., Tsushima, S., Heim, K., and Bernhard, G. (2012) Curium(III) citrate speciation in biological systems: a europium(III) assisted spectroscopic and quantum chemical study. *Dalton Trans.*, *41*, 13969-13983.
- (25) Heller, A., Barkleit, A., and Bernhard, G. (2011) Chemical Speciation of Trivalent Actinides and Lanthanides in Biological Fluids: The Dominant in Vitro Binding Form of Curium(III) and Europium(III) in Human Urine. *Chem. Res. Toxicol.*, *24*, 193-203.
- (26) Van Horn, J. D., and Huang, H. (2006) Uranium(VI) bio-coordination chemistry from biochemical, solution and protein structural data. *Coord. Chem. Rev.*, *765*-775.
- (27) Montavon, G., Apostolidis, C., Bruchertseifer, F., Repinc, U., and Morgenstern, A. (2009) Spectroscopic study of the interaction of U(VI) with transferrin and albumin

- for speciation of U(VI) under blood serum conditions. *J. Inorg. Biochem.*, *103*, 1609-1616.
- (28) Vidaud, C., Gourion-Arsiquaud, S., Rollin-Genetet, F., Torne-Celer, C., Plantevin, S., Pible, O., Berthomieu, C., and Quemeneur, E. (2007) Structural consequences of binding of  $\text{UO}_2^{2+}$  to apotransferrin: Can this protein account for entry of uranium into human cells? *Biochemistry*, *46*, 2215-2226.
  - (29) Hemadi, M., Ha-Duong, N. T., Plantevin, S., Vidaud, C., and Chahine, J. M. E. (2010) Can uranium follow the iron-acquisition pathway? Interaction of uranyl-loaded transferrin with receptor 1. *J. Biol. Inorg. Chem.*, *15*, 497-504.
  - (30) Bresson, C., Ansoborlo, E., and Vidaud, C. (2011) Radionuclide speciation: A key point in the field of nuclear toxicology studies. *J. Anal. At. Spectrom.*, *26*, 593-601.
  - (31) Basset, C., Averseng, O., Ferron, P. J., Richaud, N., Hagege, A., Pible, O., and Vidaud, C. (2013) Revision of the Biodistribution of Uranyl in Serum: Is Fetuin-A the Major Protein Target? *Chem. Res. Toxicol.*, *26*, 645-653.
  - (32) Deblonde, G. J., Sturzbecher-Hoehne, M., Mason, A. B., and Abergel, R. J. (2013) Receptor recognition of transferrin bound to lanthanides and actinides: a discriminating step in cellular acquisition of f-block metals. *Metallomics*, *5*, 619-626.
  - (33) Den Auwer, C., Llorens, I., Moisy, P., Vidaud, C., Goudard, F., Barbot, C., Solari, P. L., and Funke, H. (2005) Actinide uptake by transferrin and ferritin metalloproteins. *Radiochim. Acta*, *93*, 699-703.
  - (34) Benavides-Garcia, M. G., and Balasubramanian, K. (2009) Structural Insights into the Binding of Uranyl with Human Serum Protein Apotransferrin Structure and Spectra of Protein-Uranyl Interactions. *Chem. Res. Toxicol.*, *22*, 1613-1621.
  - (35) Vidaud, C., Dedieu, A., Basset, C., Plantevin, S., Dany, I., Pible, O., and Quemeneur, E. (2005) Screening of human serum proteins for uranium binding. *Chem. Res. Toxicol.*, *18*, 946-953.
  - (36) Ali, M., Kumar, A., Kumar, M., and Pandey, B. N. (2016) The interaction of human serum albumin with selected lanthanide and actinide ions: Binding affinities, protein unfolding and conformational changes. *Biochimie*, *123*, 117-129.
  - (37) Kumar, A., Ali, M., Ningthoujam, R. S., Gaikwad, P., Kumar, M., Nath, B. B., and Pandey, B. N. (2016) The interaction of actinide and lanthanide ions with hemoglobin and its relevance to human and environmental toxicology. *J. Hazard. Mater.*, *307*, 281-293.



- (38) Ansoborlo, E., Bion, L., Doizi, D., Moulin, C., Lourenco, V., Madic, C., Cote, G., Van der Lee, J., and Moulin, V. (2007) Current and future radionuclide speciation studies in biological media. *Radiat. Prot. Dosim.*, 127, 97-102.
- (39) Bernfeld, P. (1951) Enzymes of starch degradation and synthesis. *Advances in Enzymology and Related Subjects of Biochemistry*, 12, 379-428.
- (40) Ramasubbu, N., Ragunath, C., Sundar, K., Mishra, P. J., Gyemant, G., and Kandra, L. (2005) Structure-function relationships in human salivary alpha-amylase: role of aromatic residues. *Biologia*, 60, 47-56.
- (41) Gopal, B. A., and Muralikrishna, G. (2009) Porcine Pancreatic  $\alpha$ -Amylase and its Isoforms: Purification and Kinetic Studies. *Int. J. Food Prop.*, 12, 571-586.
- (42) Artimo, P., Jonnalagedda, M., Arnold, K., Baratin, D., Csardi, G., de Castro, E., Duvaud, S., Flegel, V., Fortier, A., Gasteiger, E., Grosdidier, A., Hernandez, C., Ioannidis, V., Kuznetsov, D., Liechti, R., Moretti, S., Mostaguir, K., Redaschi, N., Rossier, G., Xenarios, I., and Stockinger, H. (2012) ExPASy: SIB bioinformatics resource portal. *Nucleic Acids Res.*, 40, W597-W603.
- (43) Gasteiger, E., Hoogland, C., Gattiker, A., Duvaud, S., Wilkins, M. R., Appel, R. D., and Bairoch, A. (2005) Protein Identification and Analysis Tools on the ExPASy Server, In *The Proteomics Protocols Handbook* (Walker, J. M., Ed.) pp 571-607, Humana Press.
- (44) Guerra, A., Etienne-Mesmin, L., Livrelli, V., Denis, S., Blanquet-Diot, S., and Alric, M. (2012) Relevance and challenges in modeling human gastric and small intestinal digestion. *Trends Biotechnol.*, 30, 591-600.
- (45) Hill, A. V. (1910) The possible effects of the aggregation of the molecules of haemoglobin on its dissociation curves. *J. Physiol.*, 40 suppl, iv-vii.
- (46) Gans, P., Sabatini, A., and Vacca, A. (1996) Investigation of equilibria in solution. Determination of equilibrium constants with the HYPERQUAD suite of programs. *Talanta*, 43, 1739-1753.
- (47) Barkleit, A., Heller, A., Ikeda-Ohno, A., and Bernhard, G. (2016) Interaction of europium and curium with alpha-amylase. *Dalton Trans.*, 45, 8724-8733.
- (48) Guillaumont, R., Fanghänel, T., Fuger, J., Grenthe, I., Neck, V., Palmer, D. A., and Rand, M. H. (2003) *Update on the Chemical Thermodynamics of Uranium, Neptunium, Plutonium, Americium and Technetium.*, Elsevier, Amsterdam.

- (49) Pettit, L. D., Puigdomenech, I., and Wanner, H. (2004) Ionic Strength Corrections for Stability Constants using Specific Interaction Theory (SIT), Academic Software, York, UK.
- (50) Puigdomenech, I. (2013) MEDUSA and HYDRA: Software for Chemical Equilibrium Calculations, Royal Institute of Technology, Sweden.
- (51) Binstead, R. A., Zuberbühler, A. D., and Jung, B. (2005) SPECFIT Global Analysis System, version 3.0.37, Spectrum Software Associates, Marlborough, MA, USA.
- (52) Reich, T., Bernhard, G., Geipel, G., Funke, H., Hennig, C., Rossberg, A., Matz, W., Schell, N., and Nitsche, H. (2000) The Rossendorf Beam Line ROBL - a dedicated experimental station for XAFS measurements of actinides and other radionuclides. *Radiochim. Acta*, 88, 633-637.
- (53) George, G. N., and Pickering, I. J. (2000) *EXAFSPAK: a suite of computer programs for analysis of X-ray absorption spectra*. Stanford Synchrotron Radiation Laboratory, Stanford, CA.
- (54) Ankudinov, A. L., Ravel, B., Rehr, J. J., and Conradson, S. D. (1998) Real-space multiple-scattering calculation and interpretation of x-ray-absorption near-edge structure. *Phys. Rev. B*, 58, 7565-7576.
- (55) Templeton, D. H., Zalkin, A., Ruben, H., and Templeton, L. K. (1985) Redetermination and absolute-configuration of sodium uranyl(VI) triacetate. *Acta Crystallogr. Sect. C-Cryst. Struct. Commun.*, 41, 1439-1441.
- (56) Kannan, S., Barnes, C. L., and Duval, P. B. (2005) Versatile new uranyl(VI) dihalide complexes supported by tunable organic amide ligands. *Chem. Commun.*, 5997-5998.
- (57) Bernfeld, P. (1955) Amylases alpha and beta, In *Methods in Enzymology 1* (Colowick, S., and Kaplan, N., Eds.) pp 149-158, Academic Press, New York, USA.
- (58) Bernhard, G., Geipel, G., Brendler, V., and Nitsche, H. (1998) Uranium speciation in waters of different uranium mining areas. *J. Alloys Compd.*, 271-273, 201-205.
- (59) Barkleit, A., Moll, H., and Bernhard, G. (2009) Complexation of uranium(VI) with peptidoglycan. *Dalton Trans.*, 5379-5385.
- (60) Sachs, S., Brendler, V., and Geipel, G. (2007) Uranium(VI) complexation by humic acid under neutral pH conditions studied by laser-induced fluorescence spectroscopy. *Radiochim. Acta*, 95, 103-110.
- (61) Brachmann, A., Geipel, G., Bernhard, G., and Nitsche, H. (2002) Study of uranyl(VI) malonate complexation by time resolved laser-induced fluorescence spectroscopy (TRLFS). *Radiochim. Acta*, 90, 147-153.

- (62) Moulin, C., Laszak, I., Moulin, V., and Tondre, C. (1998) Time-Resolved Laser-Induced Fluorescence as a Unique Tool for Low-Level Uranium Speciation. *Appl. Spectrosc.*, 52, 528-535.
- (63) Geipel, G. (2006) Some aspects of actinide speciation by laser-induced spectroscopy. *Coord. Chem. Rev.*, 250, 844-854.
- (64) Günther, A., Steudtner, R., Schmeide, K., and Bernhard, G. (2011) Luminescence properties of uranium(VI) citrate and uranium(VI) oxalate species and their application in the determination of complex formation constants. *Radiochim. Acta*, 99, 535-541.
- (65) Moll, H., Geipel, G., Reich, T., Bernhard, G., Fanghanel, T., and Grenthe, I. (2003) Uranyl(VI) complexes with alpha-substituted carboxylic acids in aqueous solution. *Radiochim. Acta*, 91, 11-20.
- (66) Günther, A., Geipel, G., and Bernhard, G. (2007) Complex formation of uranium(VI) with the amino acids L-glycine and L-cysteine: A fluorescence emission and UV-Vis absorption study. *Polyhedron*, 26, 59-65.
- (67) Koban, A., Geipel, G., and Bernhard, G. (2003) Complex formation between uranium(VI) and alpha-D-glucose 1-phosphate. *Radiochim. Acta*, 91, 393-396.
- (68) Koban, A., Geipel, G., Rossberg, A., and Bernhard, G. (2004) Uranium(VI) complexes with sugar phosphates in aqueous solution. *Radiochim. Acta*, 92, 903-908.
- (69) Krawczyk-Bärsch, E., Lütke, L., Moll, H., Bok, F., Steudtner, R., and Rossberg, A. (2015) A spectroscopic study on U(VI) biomineralization in cultivated *Pseudomonas fluorescens* biofilms isolated from granitic aquifers. *Environ. Sci. Pollut. Res.*, 22, 4555-4565.
- (70) Reitz, T., Rossberg, A., Barkleit, A., Steudtner, R., Selenska-Pobell, S., and Merroun, M. L. (2015) Spectroscopic study on uranyl carboxylate complexes formed at the surface layer of *Sulfolobus acidocaldarius*. *Dalton Trans.*, 44, 2684-2692.
- (71) Kelly, S. D., Kemner, K. M., Fein, J. B., Fowle, D. A., Boyanov, M. I., Bunker, B. A., and Yee, N. (2002) X-ray absorption fine structure determination of pH-dependent U-bacterial cell wall interactions. *Geochim. Cosmochim. Acta*, 66, 3855-3871.
- (72) Barkleit, A., Foerstendorf, H., Li, B., Rossberg, A., Moll, H., and Bernhard, G. (2011) Coordination of uranium(VI) with functional groups of bacterial lipopolysaccharide studied by EXAFS and FT-IR spectroscopy. *Dalton Trans.*, 40, 9868-9876.

- (73) Wahlgren, U., Moll, H., Grenthe, I., Schimmelpfennig, B., Maron, L., Vallet, V., and Groen, O. (1999) Structure of uranium(VI) in strong alkaline solutions. A combined theoretical and experimental investigation. *J. Phys. Chem. A*, *103*, 8257-8264.
- (74) Safi, S., Jeanson, A., Roques, J., Solari, P. L., Charnay-Pouget, F., Den Auwer, C., Creff, G., Aitken, D. J., and Simoni, E. (2016) Thermodynamic and Structural Investigation of Synthetic Actinide-Peptide Scaffolds. *Inorg. Chem.*, *55*, 877-886.
- (75) Brulfert, F., Safi, S., Jeanson, A., Martinez-Baez, E., Roques, J., Berthomieu, C., Solari, P. L., Sauge-Merle, S., and Simoni, E. (2016) Structural Environment and Stability of the Complexes Formed Between Calmodulin and Actinyl Ions. *Inorg. Chem.*, *55*, 2728-2736.
- (76) Lahrouch, F., Chamayou, A. C., Creff, G., Duvail, M., Hennig, C., Rodriguez, M. J. L., Den Auwer, C., and Di Giorgio, C. (2017) A Combined Spectroscopic/Molecular Dynamic Study for Investigating a Methyl-Carboxylated PEI as a Potential Uranium Decorporation Agent. *Inorg. Chem.*, *56*, 1300-1308.
- (77) Denecke, M. A., Reich, T., Bubner, M., Pompe, S., Heise, K. H., Nitsche, H., Allen, P. G., Bucher, J. J., Edelstein, N. M., and Shuh, D. K. (1998) Determination of structural parameters of uranyl ions complexed with organic acids using EXAFS. *J. Alloys Compd.*, *271*, 123-127.
- (78) Pible, O., Guilbaud, P., Pellequer, J. L., Vidaud, C., and Quemeneur, E. (2006) Structural insights into protein-uranyl interaction: towards an in silico detection method. *Biochimie*, *88*, 1631-1638.
- (79) Pible, O., Vidaud, C., Plantevin, S., Pellequer, J. L., and Quemeneur, E. (2010) Predicting the disruption by  $\text{UO}_2^{2+}$  of a protein-ligand interaction. *Protein Sci.*, *19*, 2219-2230.
- (80) Wang, M., Ding, W. J., and Wang, D. Q. (2017) Binding mechanism of uranyl to transferrin implicated by density functional theory study. *RSC Adv.*, *7*, 3667-3675.
- (81) Lucks, C., Rossberg, A., Tsushima, S., Foerstendorf, H., Scheinost, A. C., and Bernhard, G. (2012) Aqueous uranium(VI) complexes with acetic and succinic acid: speciation and structure revisited. *Inorg. Chem.*, *51*, 12288-12300.
- (82) Schneyer, L. H. (1955) Inhibition of salivary amylase by uranium. *Arch. Biochem. Biophys.*, *56*, 500-506.
- (83) Bernhard, G., Geipel, G., Reich, T., Brendler, V., Amayri, S., and Nitsche, H. (2001) Uranyl(VI) carbonate complex formation: Validation of the  $\text{Ca}_2\text{UO}_2(\text{CO}_3)_3(\text{aq.})$  species. *Radiochim. Acta*, *89*, 511-518.

- (84) Sachs, S., Heller, A., Weiss, S., Bok, F., and Bernhard, G. (2015) Interaction of Eu(III) with mammalian cells: Cytotoxicity, uptake, and speciation as a function of Eu(III) concentration and nutrient composition. *Toxicol. In Vitro*, 29, 1555-1568.

## Tables

Table 1. Conditional stability constants of  $\text{UO}_2^{2+}$  with  $\alpha$ -amylase interacting with its carboxylic groups at  $I = 0.1 \text{ M}$  ( $\text{NaClO}_4$ ). The  $\log \beta^0$  values were obtained by extrapolating the  $\log \beta^{0.1}$  values to infinite dilution by applying SIT.<sup>49</sup>

Species	M L H <sup>a</sup>	$\log \beta^{0.1}$	$\log \beta^0$	Ref.
R-COOH	0 1 1	$5.23 \pm 0.14$	5.43	47
R-NH <sub>3</sub> <sup>+</sup> /R-OH	0 1 1	$10.22 \pm 0.10$	10.34	47
$\text{UO}_2[\text{R}-\text{COO}]^+$	1 1 0	$5.67 \pm 0.08$	6.07	This work
$\text{UO}_2\text{OH}[\text{R}-\text{COO}]$	1 1 -1	$0.64 \pm 0.07$	1.04	This work
$\text{UO}_2(\text{OH})_2[\text{R}-\text{COO}]^-$	1 1 -2	$-6.28 \pm 0.17$	-6.08	This work
$\text{UO}_2[\text{R}-(\text{COO})_2]$	1 2 0	$10.39 \pm 0.21$	10.98	This work

<sup>a</sup>M L H = metal / ligand / H (negative values stand for OH<sup>-</sup>)

Table 2. Summary of spectral luminescence parameters for  $\text{UO}_2^{2+}$  species relevant to this study.

Species	Peak maxima / nm						Lifetime / $\mu\text{s}$	Ref.
<i>Uranyl (aq) species</i>								
$\text{UO}_2^{2+}(\text{aq})$ pH 3.8	471.9	489.2	510.4	533.4	558.9	586.3	$1.6 \pm 0.2$	This work
$\text{UO}_2^{2+}$ pH 2.0	470.8	488.8	510.0	533.0	559.0	586.3	$1.4 \pm 0.1$	59
100 % $\text{UO}_2^{2+}$								
U(VI) pH 6.0		498	515	534	553	583	$20.9 \pm 1.5$	This work
65 % $(\text{UO}_2)_3(\text{OH})_5^+$								
15 % $\text{UO}_2\text{OH}^+$								
10 % $(\text{UO}_2)_4(\text{OH})_7^+$								
5 % $(\text{UO}_2)_2(\text{OH})_2^{2+}$								
5 % $\text{UO}_2^{2+}$								
$(\text{UO}_2)_3(\text{OH})_5^+$	484	498	514	534	557	583	$19.8 \pm 1.8$	60
$(\text{UO}_2)_4(\text{OH})_7^+$							$4.2 \pm 0.4$	60
$\text{UO}_2\text{OH}^+$	482	498	519	543	570	599	$35 \pm 2$	61
$(\text{UO}_2)_2(\text{OH})_2^{2+}$	480	497	519	542	570	598	$9 \pm 1$	62
<i>Uranyl-<math>\alpha</math>-amylase species</i>								
$\text{UO}_2[\text{R}-\text{COO}]^+$	471.6	493.1	515.1	538.5	563.4	597	$22.1 \pm 2.3$	This work
$\text{UO}_2[\text{R}-(\text{COO})_2]$	481.5	499.9	520.6	542.8	568.4	594	$7.1 \pm 1.3$	This work

Table 3. Summary of EXAFS structural parameters for  $\text{UO}_2^{2+}$  species sorbed on  $\alpha$ -amylase at different pH. Standard deviations estimated by EXAFSPAK are given in parenthesis.

Sample	Shell	N <sup>a</sup>	R <sup>b</sup> [Å]	$\sigma^2$ <sup>c</sup> [Å <sup>2</sup> ]
$\text{UO}_2^{2+}$ : $\alpha$ -amylase = 5 : 1 resp. $\text{UO}_2^{2+}$ : carboxyl = 1 : 10 initial pH = 3.5	U-O <sub>ax</sub> <sup>d</sup>	2 <sup>e</sup>	1.78(1)	0.00164
	U-O <sub>eq1</sub>	2.8(8)	2.30(2)	0.004078
	U-O <sub>eq2</sub>	1.9(4)	2.48(2)	0.004148
	U-C	1.0 <sup>f</sup>	2.84(2)	0.002 <sup>e</sup>
$\text{UO}_2^{2+}$ : $\alpha$ -amylase = 5 : 1 resp. $\text{UO}_2^{2+}$ : carboxyl = 1 : 10 initial pH = 6.0	U-O <sub>ax</sub> <sup>d</sup>	2 <sup>e</sup>	1.79(1)	0.00208
	U-O <sub>eq1</sub>	3.1(6)	2.33(2)	0.005056
	U-O <sub>eq2</sub>	1.1(6)	2.52(2)	0.001257
	U-C	0.6 <sup>f</sup>	2.93(2)	0.00603

<sup>a</sup> Errors in coordination numbers are  $\pm 25\%$ . <sup>b</sup> Errors in distance are  $\pm 0.02$  Å. <sup>c</sup> Debye-Waller factor. <sup>d</sup> The multiple scattering paths associated with the linear U-O<sub>ax</sub> arrangement were also included in the fitting. <sup>e</sup> Fixed parameters. <sup>f</sup> Linked with the N value for U-O<sub>eq2</sub> shell by assuming a bidentate coordination mode of the carboxylate group.

## Figure Legends

Figure 1. Sorption of  $\text{UO}_2^{2+}$  on  $\alpha$ -amylase as a function of pH with different uranium concentrations (left) and as a function of sorption duration (right;  $[\text{U}]_{\text{total}} = 1 \times 10^{-4} \text{ M}$  and  $\text{pH} = 6.0$ ).  $I = 0.1 \text{ M}$  with NaCl,  $T = 25 \text{ }^\circ\text{C}$ .

Figure 2. Binding isotherm of  $\alpha$ -amylase as a function of  $\text{UO}_2^{2+}$  concentration.  $[\alpha\text{-amylase}]_{\text{total}} = 0.2 - 3.0 \text{ g/L}$ ,  $\text{pH} = 6.0$ ,  $I = 0.1 \text{ M}$  with NaCl and  $T = 25 \text{ }^\circ\text{C}$ . The fitting curve was simulated according to Eq (1).

Figure 3. Species distribution of  $\text{UO}_2^{2+}$  in the presence of  $0.1 \text{ g/L}$  of  $\alpha$ -amylase ( $1.8 \times 10^{-6} \text{ M}$ , equivalent to  $9 \times 10^{-5} \text{ M}$  of carboxyl groups) with two different uranium concentrations ( $1 \times 10^{-4} \text{ M}$  relevant to the potentiometric titration experiments, and  $1 \times 10^{-5} \text{ M}$  relevant to the TRIFS measurements) as a function of pH.

Figure 4. Luminescence spectra of  $1 \times 10^{-5} \text{ M}$   $\text{UO}_2^{2+}$  in the aqueous solution containing  $0.1 \text{ g/L}$  of  $\alpha$ -amylase at pH between 2.0 and 3.0 (a, showing an increasing trend in intensity), pH between 3.0 and 8.0 (b, showing a decreasing trend in intensity), and the variation of the sum of luminescence intensity between 460 and 620 nm as a function of pH (c).

Figure 5. Luminescence spectra of two  $\text{UO}_2^{2+}$ - $\alpha$ -amylase species extracted by factor analysis.

Figure 6.  $k^3$ -weighted U  $L_{\text{III}}$ -edge EXAFS spectra of  $\text{UO}_2^{2+}$  sorbed on  $\alpha$ -amylase at different pH values (left) and their corresponding Fourier transforms (right). Black lines; experimental data, red lines; theoretical fitting.

Figure 7. Enzyme activity of  $\alpha$ -amylase as a function of uranium concentration without- (purple) and with (green) an excess of  $\text{Ca}^{2+}$ .  $[\text{Ca}^{2+}]_{\text{total}} = 10^{-3} \text{ M}$ . Enzyme activity without metal ions relates to 100 %.



## Figures

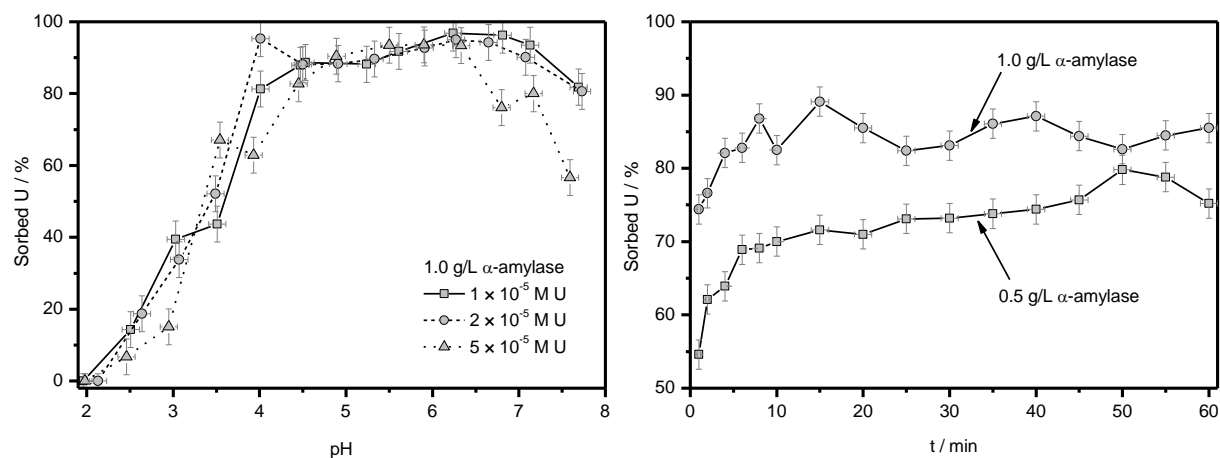


Figure 1. Sorption of  $\text{UO}_2^{2+}$  on  $\alpha$ -amylase as a function of pH with different uranium concentrations (left) and as a function of sorption duration (right;  $[\text{U}]_{\text{total}} = 1 \times 10^{-4}$  M and pH = 6.0).  $I = 0.1$  M with NaCl,  $T = 25$  °C.

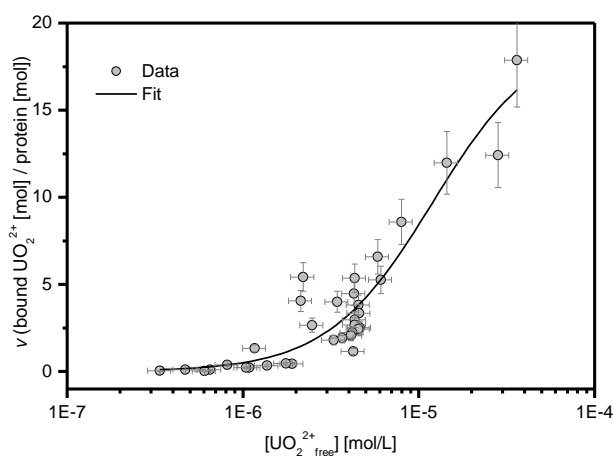


Figure 2. Binding isotherm of  $\alpha$ -amylase as a function of  $\text{UO}_2^{2+}$  concentration.  $[\alpha\text{-amylase}]_{\text{total}} = 0.2 - 3.0$  g/L, pH = 6.0,  $I = 0.1$  M with NaCl and  $T = 25$  °C. The fitting curve was simulated according to Eq (1).

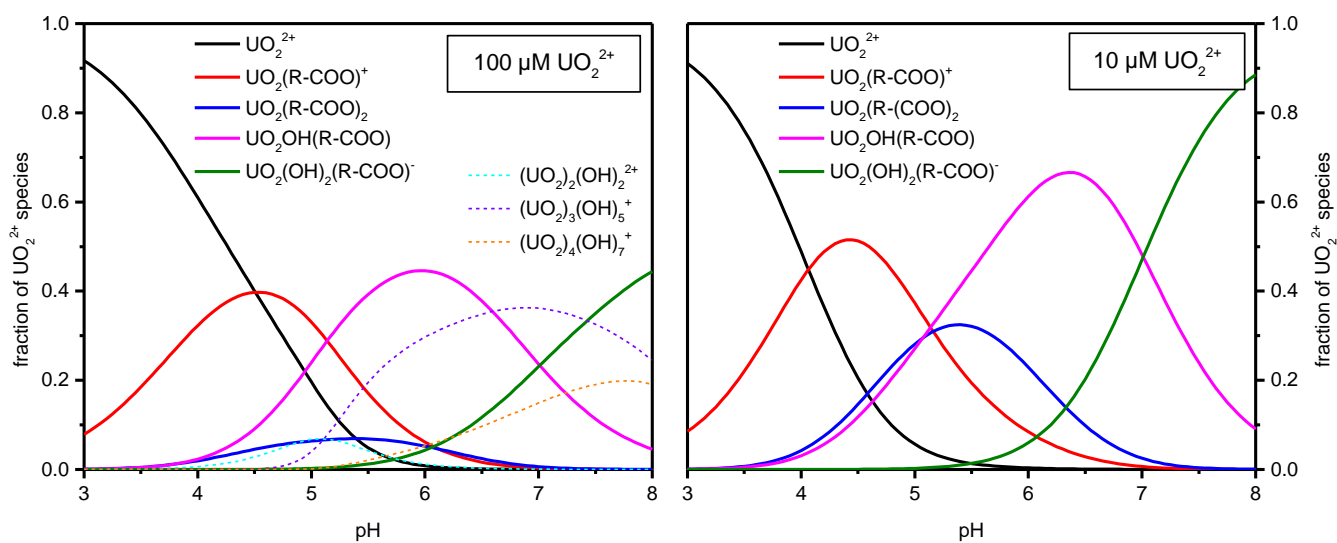


Figure 3. Species distribution of  $\text{UO}_2^{2+}$  in the presence of 0.1 g/L of  $\alpha$ -amylase ( $1.8 \times 10^{-6}$  M, equivalent to  $9 \times 10^{-5}$  M of carboxyl groups) with two different uranium concentrations ( $1 \times 10^{-4}$  M relevant to the potentiometric titration experiments, and  $1 \times 10^{-5}$  M relevant to the TRLFS measurements) as a function of pH.

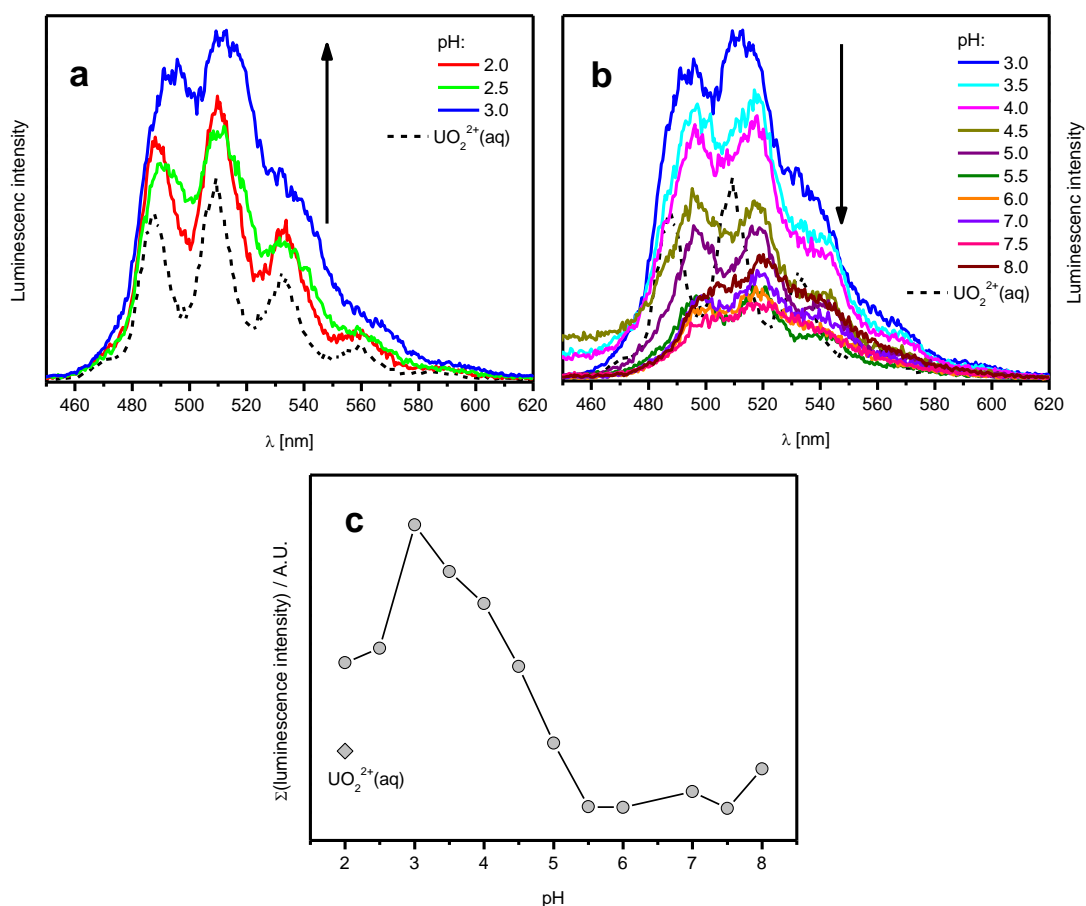


Figure 4. Luminescence spectra of  $1 \times 10^{-5} \text{ M } \text{UO}_2^{2+}$  in the aqueous solution containing 0.1 g/L of  $\alpha$ -amylase at pH between 2.0 and 3.0 (a, showing an increasing trend in intensity), pH between 3.0 and 8.0 (b, showing a decreasing trend in intensity), and the variation of the sum of luminescence intensity between 460 and 620 nm as a function of pH (c).

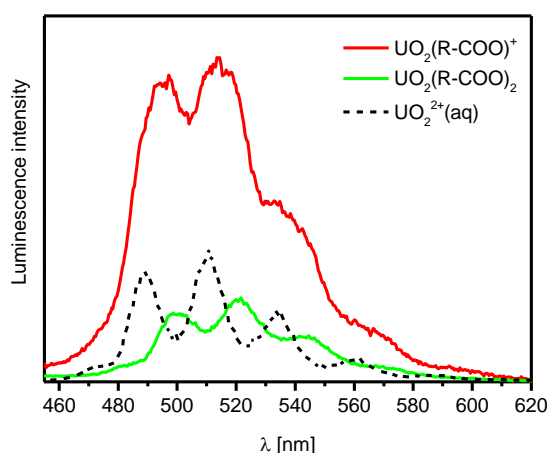


Figure 5. Luminescence spectra of two  $\text{UO}_2^{2+}$ - $\alpha$ -amylase species extracted by factor analysis.

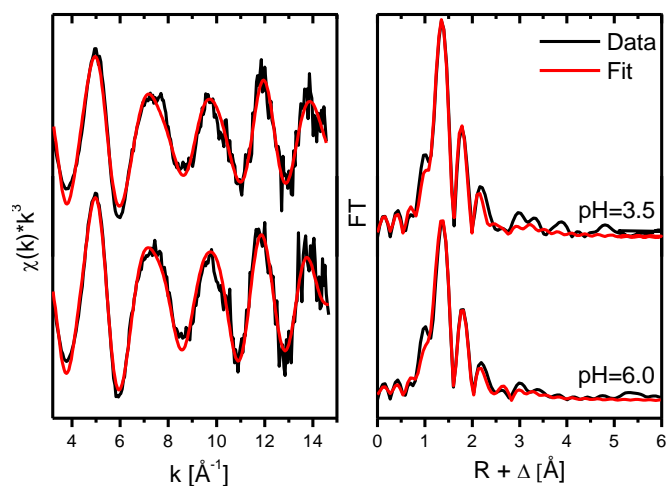


Figure 6.  $k^3$ -weighted U  $L_{III}$ -edge EXAFS spectra of  $UO_2^{2+}$  sorbed on  $\alpha$ -amylase at different pH values (left) and their corresponding Fourier transforms (right). Black lines; experimental data, red lines; theoretical fitting.

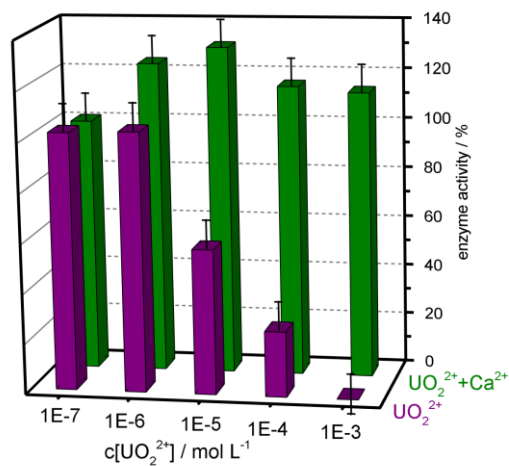


Figure 7. Enzyme activity of  $\alpha$ -amylase as a function of uranium concentration without- (purple) and with (green) an excess of  $Ca^{2+}$ .  $[Ca^{2+}]_{total} = 10^{-3}$  M. Enzyme activity without metal ions relates to 100 %.